© 2017. Published by The Company of Biologists Ltd | Journal of Cell Science (2017) 130, 735-744 doi:10.1242/jcs.196014

RESEARCH ARTICLE

Role of the phagosomal redox-sensitive TRP channel TRPM2 in regulating bactericidal activity of macrophages

Anke Di*, Tomohiro Kiya*, Haixia Gong, Xiaopei Gao and Asrar B. Malik‡

ABSTRACT

Acidification of macrophage phagosomes serves an important bactericidal function. We show here that the redox-sensitive transient receptor potential (TRP) cation channel TRPM2 is expressed in the phagosomal membrane and regulates macrophage bactericidal activity through the activation of phagosomal acidification. Measurement of the TRPM2 current in phagosomes identified TRPM2 as a functional redox-sensitive cation channel localized in the phagosomal membrane. Simultaneous measurements of phagosomal Ca^{2+} changes and phagosome acidification in macrophages undergoing phagocytosis demonstrated that TRPM2 was required to mediate the efflux of cations and for phagosomal acidification during the process of phagosome maturation. Acidification in phagosomes was significantly reduced in macrophages isolated from *Trpm2*$^{-/-}$ mice as compared to wild type, and acidification was coupled to reduced bacterial clearance in *Trpm2*$^{-/-}$ mice. *Trpm2*$^{+/+}$ macrophages treated with the vacuolar H^+-ATPase inhibitor bafilomycin showed reduced bacterial clearance, similar to that in *Trpm2*$^{-/-}$ macrophages. Direct activation of TRPM2 using adenosine diphosphate ribose (ADPR) induced both phagosomal acidification and bacterial killing. These data collectively demonstrate that TRPM2 regulates phagosomal acidification, and is essential for the bacterial killing function of macrophages.

KEY WORDS: Bactericidal activity, Ion channel, Phagosome

INTRODUCTION

Macrophages, upon ingesting invading micro-organisms, have the primary function of killing bacteria through maturation of phagosomes as defined by their acidification (Russell et al., 2009; Vieira et al., 2002). The mature phagosome is also rich in proteolytic enzymes, ensuring effective degradation of internalized microbes (Kinchen and Ravichandran, 2008). During phagosome maturation, phagosomes recruit vacuolar proton (H^+)-ATPases (vATPases) that transfer H^+ into phagosomes (Flannagan et al., 2009). To optimize H^+ accumulation, efflux of cations and influx of anions such as chloride (Hara-Chikuma et al., 2005) are needed to dissipate the development of a restrictive electrical gradient induced by the H^+ influx (Steinberg et al., 2007a). However, the identity of these channels remains unclear (Steinberg et al., 2010).

Department of Pharmacology and the Center for Lung and Vascular Biology, The University of Illinois College of Medicine, Chicago, IL 60612, USA.
*These authors contributed equally to this work

‡Author for correspondence (abmalik@uic.edu)

A.D., 0000-0001-5055-1407; T.K., 0000-0003-0027-7758; A.B.M., 0000-0002-8205-7128

Received 27 July 2016; Accepted 21 December 2016

Transient receptor potential melastatin 2 (TRPM2), a redox-sensitive non-selective cation channel localized in the plasma membrane (Hara et al., 2002; Knowles et al., 2013; Perraud et al., 2001, 2005; Syed Mortadza et al., 2015; Toth and Csanady, 2010), plays an important role in bacterial clearance due in part to its ability to activate cytokine generation (Knowles et al., 2011; Qian et al., 2014). Impaired production of cytokines in *Trpm2*$^{-/-}$ mice led to high mortality following *Listeria monocytogenes* (*LM*) challenge (Knowles et al., 2011). TRPM2 may also control the killing of internalized *Escherichia coli* through its role as a plasma membrane Ca^{2+}-influx channel and induce phagosome–lysosome fusion (Zhang et al., 2017). Because of the importance of macrophages in killing bacteria, here, we addressed the question of whether TRPM2 is expressed in phagosomal membrane of macrophages and whether it functions as an efflux of cation channel to regulate phagosomal pH and thereby bacterial killing.

RESULTS

TRPM2-mediated killing of bacteria in macrophages

Studies using TRPM2-knockout (*Trpm2*$^{-/-}$) mice have previously shown that the protective role of TRPM2 in polymicrobial sepsis (Qian et al., 2014) and *Listeria monocytogenes* (*LM*) infection (Knowles et al., 2011) is mediated by TRPM2-dependent bacterial clearance. However, the question remains as to whether TRPM2 is expressed in phagosomes of macrophages and whether its phagosomal expression contributes to bacterial killing. Here, we studied the role of TRPM2 in phagosomes of macrophages for killing of the gram-negative bacteria *Pseudomonas aerugenosa* (*PA*), a common pathogen mediating respiratory infection (Sadikot et al., 2005). We first examined the role of TRPM2 in mice challenged intra-tracheally with *PA*. We observed markedly augmented lung *PA* retention in *Trpm2*$^{-/-}$ compared to in *Trpm2*$^{+/+}$ mice (Fig. 1A). Mortality was also greater in *Trpm2*$^{-/-}$ relative to *Trpm2*$^{+/+}$ mice in response to intra-tracheal administration of *PA* as well as to cecal ligation puncture (CLP), a model of polymicrobial sepsis (Fig. 1B,C). We next determined whether TRPM2 in isolated macrophages contributed to killing of *PA*. Upon infecting mouse bone marrow-derived macrophages (BMDMs) with either gram-negative *PA* bacteria or gram-positive *Staphylococcus aureus* (*SA*) bacteria, we observed significantly greater bacterial survival in BMDMs from *Trpm2*$^{-/-}$ mice exposed to *PA* or *SA* than BMDMs from *Trpm2*$^{+/+}$ mice (Fig. 1D,E).

Distribution of TRPM2 in phagosomes

Although TRPM2 is known to be expressed in the plasma membrane of macrophages (Di et al., 2011), its distribution in phagosomes is unclear. We identified marked TRPM2 immunostaining in human alveolar macrophages (Fig. 2A–C, green). We also demonstrated, by feeding human alveolar macrophages latex beads, that TRPM2 was specifically distributed in the phagosome membrane (Fig. 2D). Furthermore, TRPM2

Journal of Cell Science

Journal of Cell Science (2017) 130, 735-744 doi:10.1242/jcs.196014

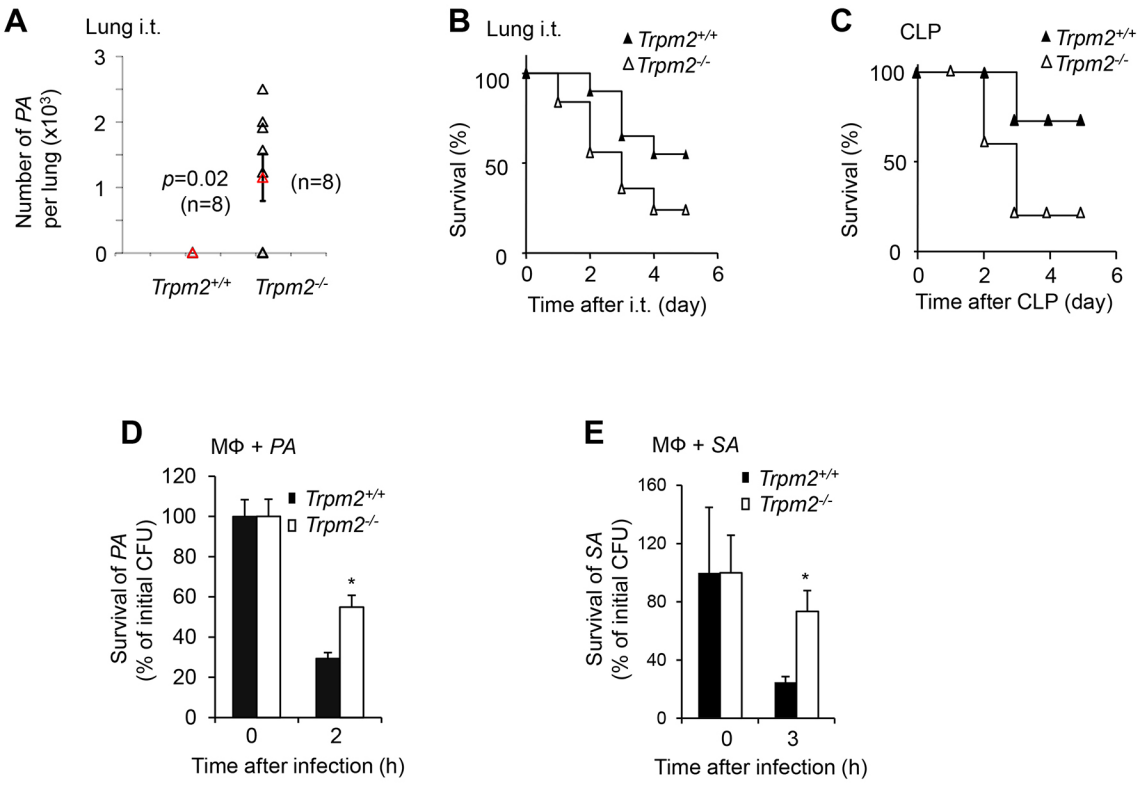

Fig. 1. TRPM2 deletion in mice augments sepsis-induced mortality and increases bacteria survival in lungs and macrophages. (A) TRPM2 deletion reduced bacterial killing in murine lungs. *Trpm2*$^{+/+}$ and *Trpm2*$^{-/-}$ mice were challenged by intra-tracheal instillation (*i.t.*) with *PA* (10^5 per mouse), and lungs were removed aseptically 48 h after infection and homogenized. Diluted homogenates were plated and number of colonies was counted after incubation for 18 h at 37°C. Data are displayed using scatter points; the mean±s.e.m. (red) is also shown. Differences between *Trpm2*$^{+/+}$ and *Trpm2*$^{-/-}$ were determined by *t*-test (P<0.05, n=8 in each group). (B,C) TRPM2 ablation increases sepsis-induced mortality in mice. Mouse survival was determined after *PA* lung infection either intra-tracheally (10^5 per mouse) (B) or through CLP (C). Differences in mortality were determined by a log-rank test as P<0.05 (n=25, B; n=10, C). (D,E) TRPM2 deletion increases *PA* and *SA* survival in bone marrow-derived macrophages (MΦ). BMDMs exposed to *PA* for 30 min with a MOI of 20 (D) or exposed to *SA* for 30 min with MOI of 10 (E). Results are mean±s.e.m. (n=3). *P<0.05 compared with *Trpm2*$^{+/+}$ macrophages (*t*-test).

staining was seen in phagosomes of BMDMs from *Trpm2*$^{+/+}$ but not in *Trpm2*$^{-/-}$ mice (Fig. 2E–I). Since lysosomes contribute to phagosomal maturation (Flannagan et al., 2009; Vieira et al., 2002), we next determined whether TRPM2 is present in lysosomes. Macrophages were immunostained with anti-TRPM2 antibody and antibody against the lysosome marker lysosomal-associated membrane protein 1 (LAMP1) (Meikle et al., 1997). However, we observed that TRPM2 staining was absent in lysosomes (Fig. S1).

Activation of TRPM2 in phagosomes

We next used patch clamping to monitor the current in phagosomes isolated from BMDMs (Samie et al., 2013). ADP-ribose (ADPR; 200 µM) was added to the patch pipette solution to activate TRPM2 (Perraud et al., 2001). ADPR activated a non-selective phagosomal cation current with a linear current–voltage plot, and isosmotic replacement of external Na^+ with the impermeant organic cation N-methyl-D-glucamine (NMDG) abolished the inward current (Fig. 3A–C). Phagosomes from *Trpm2*$^{-/-}$ BMDMs failed to respond to ADPR (Fig. 3C). ADPR added to the bath solution also failed to activate a current (Fig. 3A–C). These findings demonstrated the intra-luminal localization of the TRPM2 C- and N-terminals. Since TRPM2 is a redox-sensitive channel (Hara et al., 2002; Perraud et al., 2005), it can also be activated by oxidants (Wehage et al., 2002). We showed that H_2O_2 (100 µM) added into phagosomes via the micropipette elicited a non-selective cation current in *Trpm2*$^{+/+}$ BMDMs and isosmotic replacement of external Na^+ by NMDG significantly reduced the inward current, but not the outward current (Fig. 3D–F). Furthermore, the H_2O_2-induced current was significantly reduced in *Trpm2*$^{-/-}$ BMDMs.

Since there is uncertainty about whether oxidants and oxidant-mediated production of ADPR activate TRPM2 (Knowles et al., 2013), we next examined whether H_2O_2-induced activation of TRPM2 occurred secondary to production of ADPR. We observed that 8-Br-ADPR (an antagonistic analog of ADPR; Partida-Sanchez et al., 2007) reduced H_2O_2-induced current in *Trpm2*$^{+/+}$ BMDMs to the level seen in *Trpm2*$^{-/-}$ BMDMs (Fig. 3D–F). However, 8-Br-ADPR did not modify the H_2O_2-induced current in *Trpm2*$^{-/-}$ BMDMs (Fig. 3D–F), consistent with the essential role of generation of H_2O_2 in activating phagosomal TRPM2 secondary to ADPR generation.

We next addressed the postulated mechanism by which reactive oxygen species (ROS) induced production of ADPR in phagosomes. The mechanism involves H_2O_2-induced generation of ADPR through the oxidant sensitive-enzyme NADase (also known as NAD glycohydrolase), which catalyzes hydrolysis of NAD into ADPR (Albeniz et al., 2004), and poly(ADP-ribose) polymerase (PARP), which binds single-stranded and double-stranded DNA breaks and catalyzes breakdown of NAD into poly-ADPR (Fonfria et al., 2004; Hecquet and Malik, 2009). We observed in patch clamp experiments that included nicotinamide, an inhibitor of NADase (Alano et al., 2010), along with H_2O_2 in the intra-phagosomal pipette solution did not show a H_2O_2-activated

Journal of Cell Science (2017) 130, 735-744 doi:10.1242/jcs.196014

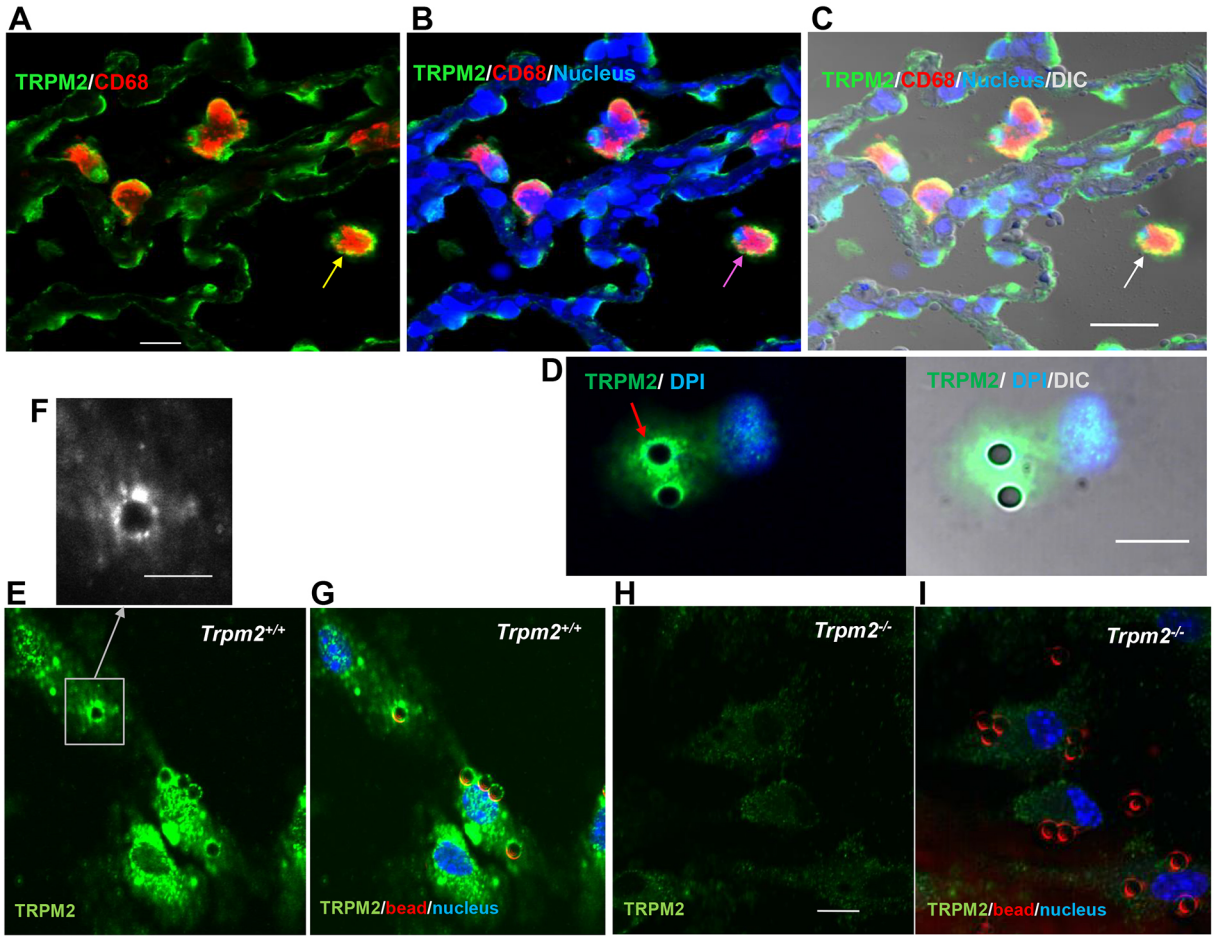

Fig. 2. TRPM2 distribution in lungs, macrophages and phagosomes. (A–C) Confocal images of TRPM2 immunostaining in human lung sections. Tissue from cadaveric human lungs were fixed with formalin and paraffin embedded (FFPE). TRPM2 (green) in lung sections (5 µm) was identified with rabbit anti-human TRPM2 antibody. Human alveolar macrophages (arrows, red) were identified with anti-CD68 antibody. (D) Confocal images of TRPM2 immunostaining in phagosomes of isolated human alveolar macrophages. Phagosomes are seen inside macrophages following phagocytosis of polystyrene particles (3 µm). The ring-like staining of TRPM2 in phagosomes is indicated by a red arrow. (E–I) Confocal images of TRPM2 immunostaining in phagosomes of mouse BMDM from *Trpm2*$^{+/+}$ mice (E,G) and *Trpm2*$^{-/-}$ mice (H,I). Phagosomes are seen inside macrophage following phagocytosis of polystyrene particles (3 µm). To make the beads clearer, we have added false color (red) to beads using software by changing gray the DIC image into a red DIC image. A ring-like staining of TRPM2 in phagosomes of BMDMs from *Trpm2*$^{+/+}$ mice is seen (E,G) and shown in higher resolution in F. There was no TRPM2 staining in BMDM from *Trpm2*$^{-/-}$ mice (H,I). Rabbit polyclonal antibody against TRPM2 was used. Scale bars: 20 µm (A–C); 10 µm (E,G–I); 5 µm (D,F).

current (Fig. 3E,F). Thus, oxidant-induced ADPR generation in phagosomes involved oxidant-sensitive transition of NAD into ADPR mediated by NADase.

Coupling of phagosomal TRPM2 activation and phagosomal acidification in macrophage during phagosome maturation

Since phagosomal TRPM2 faces the inner aspect of the phagosome, as evident by the electrophysiological measurements described above (Fig. 3), we next determined the relationship between TRPM2 recruitment to the phagosome and phagosomal acidification during phagosome maturation. In this study, we simultaneously monitored both phagosomal TRPM2 activation and acidification. Intra-phagosomal Ca^{2+} was determined using fluo3 and phagosomal acidification was determined using the pH-sensitive fluorescent dye pHrodoRed (hereafter pHrodo) conjugated to *SA* (Fig. 4). We observed greater intra-phagosomal Ca^{2+} accumulation (a green fluorescence increase) in *Trpm2*$^{-/-}$ mouse (m)BMDMs compared to *Trpm2*$^{+/+}$ mBMDMs during phagosomal acidification (Fig. 4A,C; Movies 1,2). Further, we observed weaker increase in intensity of fluorescence from pHrodo in *Trpm2*$^{-/-}$ BMDMs as compared to *Trpm2*$^{+/+}$ BMDMs (Fig. 4A,D; Movies 1,2), indicating decreased phagosomal acidification in *Trpm2*$^{-/-}$ macrophages. These findings thus demonstrate that TRPM2 activation, as reflected by efflux of Ca^{2+} in *Trpm2*$^{+/+}$ BMDMs, occurred in parallel with phagosomal acidification.

Impaired phagosomal acidification in *Trpm2*$^{-/-}$ macrophage causes defective killing of bacteria

To further evaluate the role of TRPM2 in regulating phagosomal pH, we also measured phagosomal pH using dual fluorescence flow cytometry (Sokolovska et al., 2012). *SA* was conjugated to ratiometric fluorescent dyes containing both the pH-sensitive component Oregon Green 488 (OG), having a low pK_a (4.8) (Han and Burgess, 2010), and the acidification-insensitive component carboxy-tetramethyl-rhodamine (TAMRA) (Sokolovska et al., 2012) (Fig. 5A). The intensity ratios of OG and TAMRA versus pH were obtained by flow cytometry. Calibration of fluorescence was interpolated on a standard curve for the intensity ratios of OG and TAMRA versus pH determined *in vitro* using a series of buffers (Fig. 5A,B). BMDMs containing *SA* from *Trpm2*$^{-/-}$ mice showed

Journal of Cell Science (2017) 130, 735-744 doi:10.1242/jcs.196014

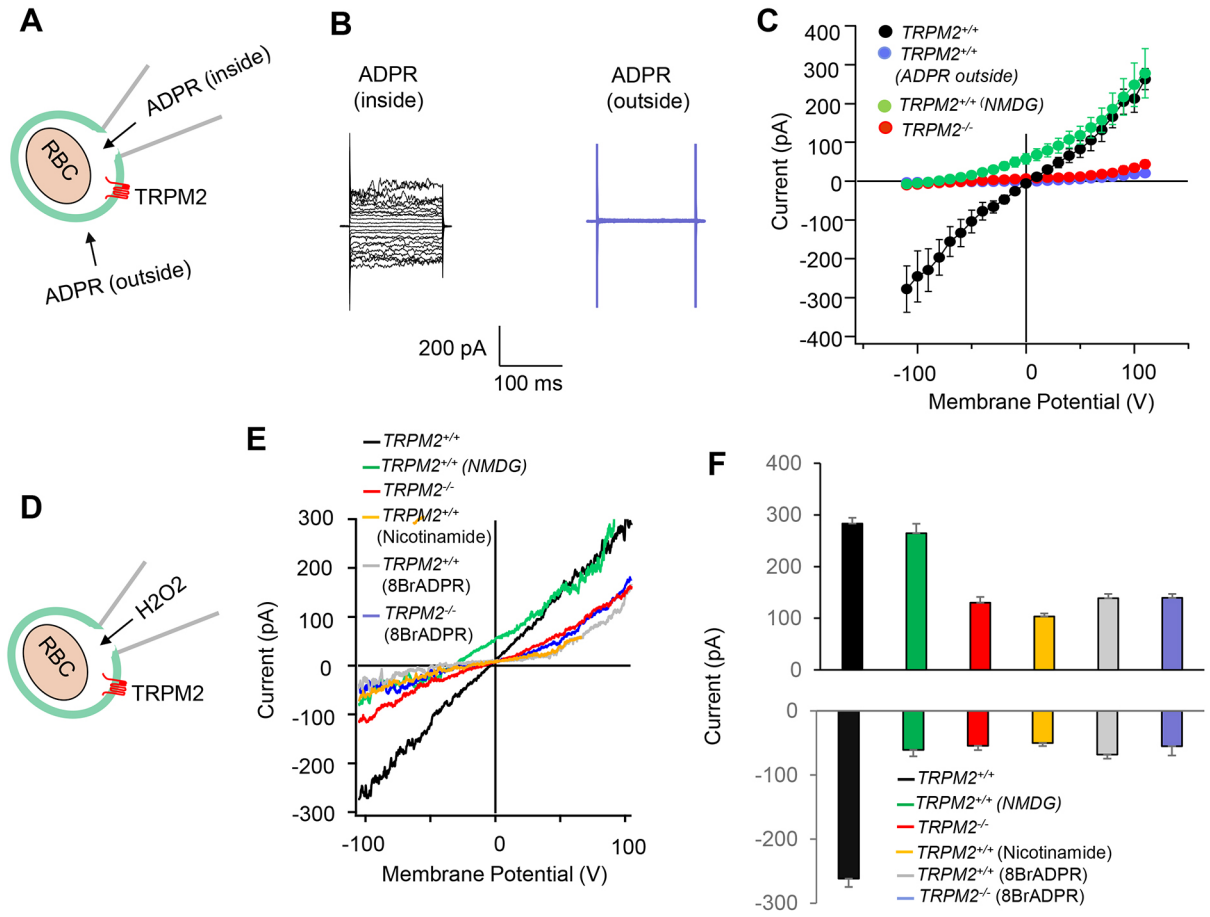

Fig. 3. Electrophysiological recording of TRPM2 activation in isolated phagosomes. (A–C) Patch clamp analysis of whole-phagosome current induced by ADPR. An illustration of the whole-phagosome configuration with ADPR added in the pipette solution (inside) and ADPR added in the bath solution (outside) is shown in A. A patch pipette was used to slice open the macrophage and to release RBC-containing phagosomes. A new patch pipette was then used to achieve the whole-phagosome configuration as described previously (Samie et al., 2013). Representative raw currents are displayed in B and the average (mean±s.e.m.) of *I–V* (current–voltage) plot based on the raw currents is displayed in C (n=5). Currents induced by ADPR (200 µM, added in the pipette solution – 'inside') is shown in black and currents induced by ADPR (with same concentration, added in the bath solution – 'outside') is shown in blue for *Trpm2*$^{+/+}$ phagosomes. ADPR added in the pipette solution for phagosomes from *Trpm2*$^{-/-}$ BMDMs significantly (P<0.05) reduced the whole phagosome current (shown in red in C). Note the inhibition of the inward current and the left-shift of reversal potential for the ADPR-induced current in *Trpm2*$^{+/+}$ phagosomes when Na^+ is replaced with NMDG (green curve in C). (D–F) Patch clamp analysis of whole-phagosome current induced by H_2O_2. In these experiments, 100 µM H_2O_2 was added in the pipette solution to induce TRPM2 activation in the isolated phagosomes as illustrated in D. *I–V* plots of H_2O_2-induced currents with a ramp protocol (range from −105 mV to +105 mV within 200 ms) are shown in E and the averaged (mean±s.e.m.) amplitude of current at −105 mV and +105 mV is shown in F (n=5). Note the significantly (P<0.05) reduced currents induced by H_2O_2 in *Trpm2*$^{-/-}$ phagosomes (red) compared with the one in *Trpm2*$^{+/+}$ phagosomes (black). Both 8-Br-ADPR (10 µM, added in the pipette solution, gray) and nicotinamide (200 µM, added in the pipette solution, orange) reduced H_2O_2 current in *Trpm2*$^{+/+}$ phagosomes to the same level seen in *Trpm2*$^{-/-}$ phagosomes (red). 8-Br-ADPR did not affect the H_2O_2-induced current in *Trpm2*$^{-/-}$ phagosomes (blue).

greater pH values (6.53±0.28, mean±s.e.m.) in phagosomes containing *SA* than the *Trpm2*$^{+/+}$ BMDMs (5.32±0.01) measured after phagocytosis (Fig. 5C). *Trpm2*$^{+/+}$ BMDMs treated with diphenyleneiodonium (DPI; an inhibitor of NOX) (Cross and Jones, 1986), however, showed increased phagosomal pH (6.71±0.46) similar to the pH value (6.87±0.12) of phagosomes from *Trpm2*$^{-/-}$ BMDMs treated with DPI (Fig. 5D). These findings together show the central role of oxidant-mediated TRPM2 activation in the mechanism of phagosomal pH drop.

To address whether defective phagosomal acidification was responsible for the *PA*-killing defect seen in *Trpm2*$^{-/-}$ macrophages (Fig. 1), we next determined *PA* killing following treatment of BMDMs with bafilomycin, which inhibits H^+ influx (Lukacs et al., 1990). Bafilomycin-treated macrophages from *Trpm2*$^{+/+}$ mice showed significantly greater *PA* survival than control untreated cells, and moreover, the level of bacterial killing was similar to *Trpm2*$^{-/-}$ BMDM (Fig. 5E).

We next examined phagosomal acidification and bacterial killing in the presence of 8-Br-ADPR, an analog of ADPR (Partida-Sanchez et al., 2007) that does not activate TRPM2. Phagosomal pH and bacterial survival increased in *Trpm2*$^{+/+}$ BMDMs treated with 8-Br-ADPR to the same extent as seen in *Trpm2*$^{-/-}$ BMDMs (Fig. 5F,G). These observations showed that oxidant-mediated ADPR production was essential for the TRPM2 activation in phagosomes and thereby for bacterial killing by macrophages (Fig. 5H).

Since the fusion of lysosomes with phagosomes may regulate phagosomal pH (Vieira et al., 2002), we next queried whether phagosomal TRPM2 was involved in the fusion process. Phagosomes were traced by pHrodo conjugated to *SA* and lysosomes were traced with the fluorescent dye Alexa Fluor 488 conjugated to dextran as described previously (Steinberg et al., 2010). We first examined phagosomes positive for dextran–Alexa-Fluor-488 staining as the percent of all phagosomes detected by

Journal of Cell Science (2017) 130, 735-744 doi:10.1242/jcs.196014

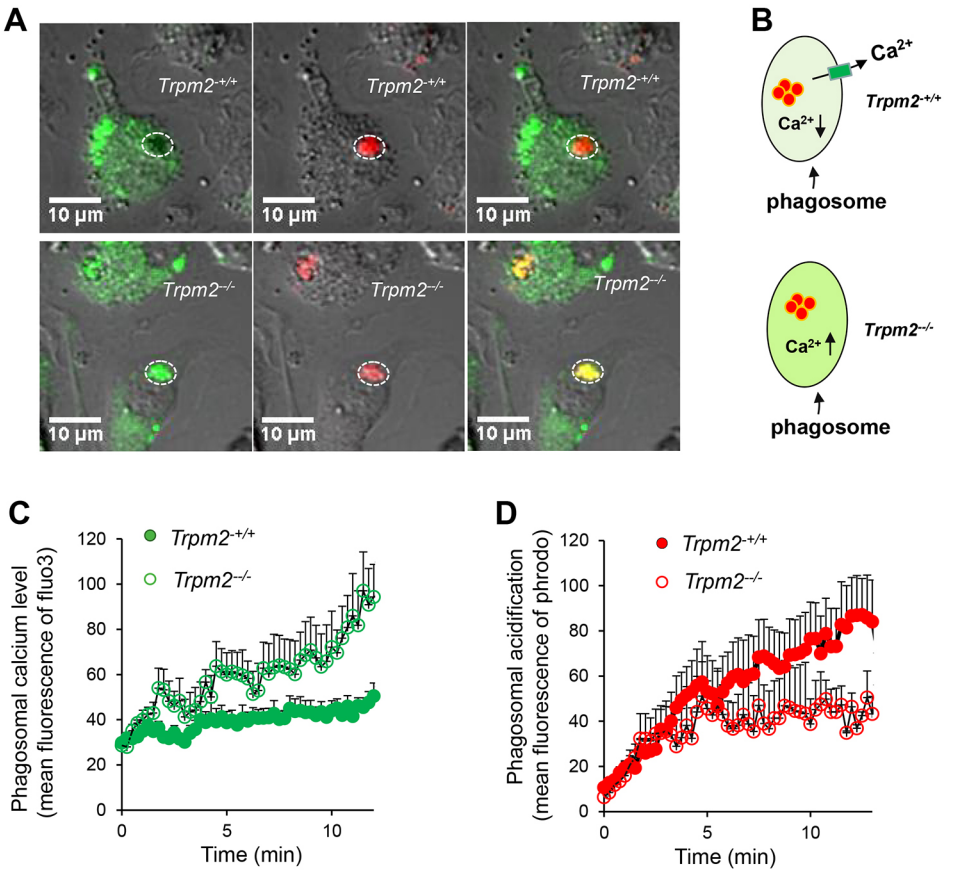

Fig. 4. Simultaneous recordings of phagosomal TRPM2 activation and phagosomal acidification. Phagosomal TRPM2 activation was monitored by recording changes in intra-phagosomal Ca^{2+} using fluo3, and phagosomal acidification was monitored in phagosomes containing *SA* conjugated to the pH-sensitive fluorescent dye pHrodo. (A,B) Images showing a higher intra-phagosomal Ca^{2+} concentration (A, indicated by stronger green color and yellow staining) in *Trpm2*$^{-/-}$ BMDMs as compared with *Trpm2*$^{+/+}$ BMDMs (as illustrated in B). The images also show that there is reduced phagosomal acidification in *Trpm2*$^{-/-}$ BMDMs as evident by the weaker intensity of pHrodo fluorescence (red color) compared with that in *Trpm2*$^{+/+}$ BMDMs. (C) The intra-phagosomal Ca^{2+} changes were traced by measuring the mean intensity of fluo3 fluorescence for each phagosome over time with Fuji software (means±s.e.m., n=4, P<0.05 compared with *Trpm2*$^{-/-}$ macrophage; *t*-test). Also see live-cell video recordings of these changes in Movies 1 and 2. (D) The level of pHrodo fluorescence for images such as those shown in A was analyzed quantitatively over time (means±s.e.m., n=4).

staining with pHrodo. We then examined the strength of lysosome fluorescence (Alexa Fluor 488) of each phagosome containing pHrodo fluorescence (Fig. S2). However, we did not observe any difference in the fluorescence intensity distribution of the lysosomal dye (Alexa Fluor 488) for each phagosome containing pHrodo, or a difference in proportion the phagosomes positive for dextran–Alexa-Fluor-488 staining as a percentage of all phagosomes detected between *Trpm2*$^{+/+}$ and *Trpm2*$^{-/-}$ mBMDMs (Fig. S2G,H). Phagosomes containing *SA* from *Trpm2*$^{+/+}$ and *Trpm2*$^{-/-}$ mBMDMs showed similar loading of dextran (Fig. S2G,H). These studies demonstrated no fusion defect in either group.

DISCUSSION

Macrophages serve as an essential host-defense function in killing invading bacteria secondary to phagosomal maturation and decrease in pH (Vieira et al., 2002). We previously showed that TRPM2 functioning as a non-selective cation channel at the plasma membrane of macrophages increased survival of endotoxemic mice and decreased inflammatory lung injury secondary to activation of influx of cations and depolarization of the plasma membrane (Di et al., 2011). However in the present study, in profiling TRPM2 expression in macrophages, we also found that TRPM2 was present in the phagosomal membrane. Furthermore, we showed that the phagosomally distributed TRPM2 was required for killing gram-negative bacteria *PA* and gram-positive bacteria *SA* secondary to promoting acidification of phagosomes. Specifically, macrophage phagosomes obtained from *Trpm2*$^{-/-}$ mice failed to acidify, and treatment of *Trpm2*$^{+/+}$ macrophages with the vATPase inhibitor bafilomycin showed the same *PA*-killing defect as seen in *Trpm2*$^{-/-}$ macrophages. Furthermore, macrophages treated with the TRPM2 antagonist 8-Br-ADPR (Partida-Sanchez et al., 2007), which, unlike ADPR, fails to bind TRPM2 in the C-terminal NUDT9-H (ADPRase) domain of the channel (Perraud et al., 2001), displayed the same defects in phagosomal acidification and bacterial killing as seen in *Trpm2*$^{-/-}$ macrophages. These results collectively demonstrated an essential role of phagosomal TRPM2 in killing bacteria secondary to phagosomal acidification.

Zhan et al. have also observed defective *E. coli* killing in stimulated peritoneal *Trpm2*$^{-/-}$ macrophages, which they ascribed to defective phagosome–lysosome fusion resulting from impaired Ca^{2+} influx via the plasma membrane-localized TRPM2 (Zhang et al., 2017). In the present study however, on carefully examining the distribution and function of TPRM2, we observed localization of TRPM2 in phagosomes but not in lysosomes of macrophages derived from bone marrow. We demonstrated that the impaired phagosomal acidification and bacteria killing of *Trpm2*$^{-/-}$ macrophages were due solely to the lack of counter conductance for proton influx. Furthermore, phagosome–lysosome fusion in both *Trpm2*$^{+/+}$ and *Trpm2*$^{-/-}$ BMDMs was similar, indicating that the defective phagosome–lysosome fusion in the present study cannot explain the impaired killing defect of *Trpm2*$^{-/-}$ macrophages. The reasons for the discrepancy in the findings are not clear. One possibility is that the stimulated peritoneal macrophages used by Zhang et al. (2017) may have been activated prior to their use, and thus this favored fusion of phagosomes and lysosomes.

In a previous study addressing the role of TRPM2-mediated inhibition of ROS generation (Di et al., 2011), augmented *E. coli.* killing was observed in lungs and blood of *Trpm2*$^{-/-}$ compared to *Trpm2*$^{+/+}$ mice after a 4 h period of infection, whereas there was no difference between *Trpm2*$^{+/+}$ and *Trpm2*$^{-/-}$ mice seen at 24 h after infection. In the study using mice infected with *LM*, the liver and spleen bacterial killing in *Trpm2*$^{-/-}$ was less than in *Trpm2*$^{+/+}$ mice

Journal of Cell Science (2017) 130, 735-744 doi:10.1242/jcs.196014

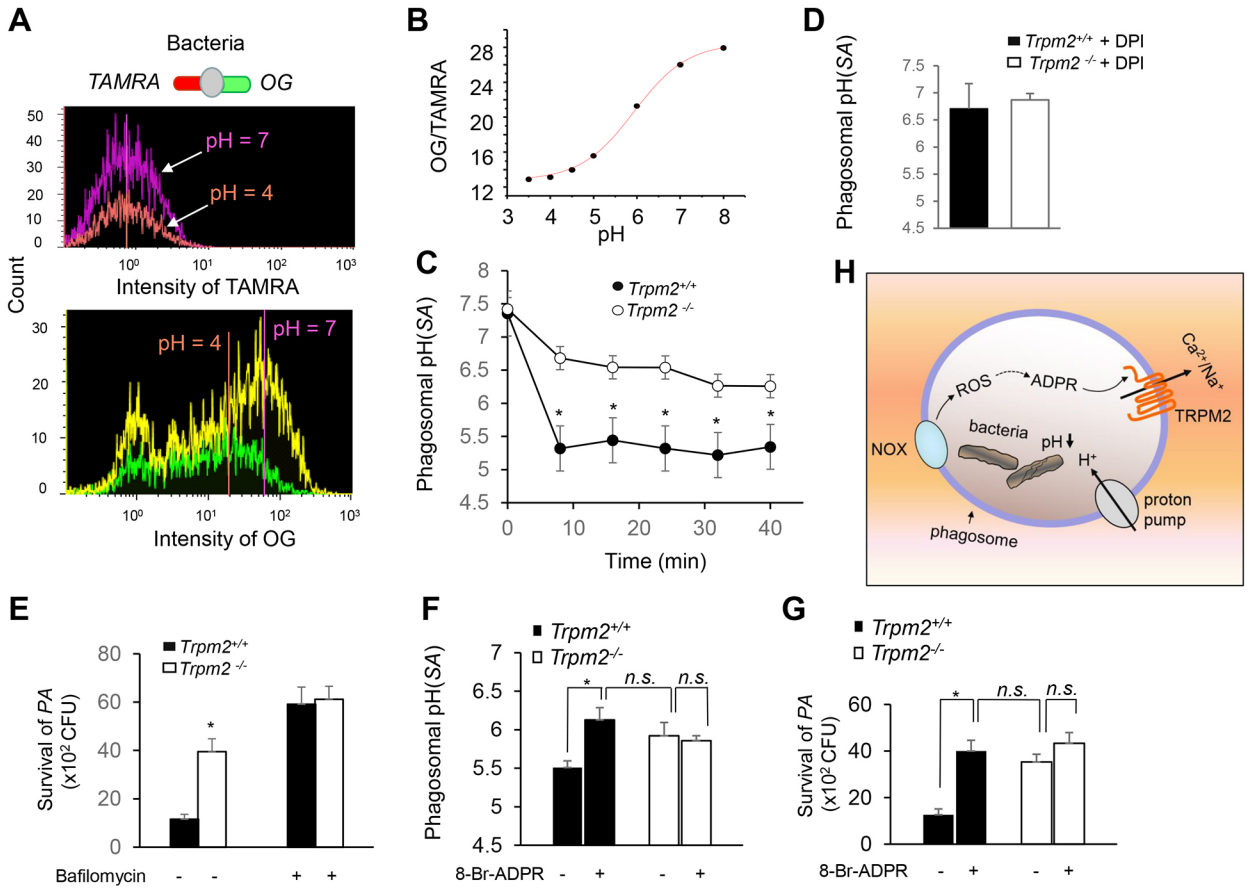

Fig. 5. TRPM2 regulates phagosomal acidification and the bacterial killing function of macrophages. (A–C) BMDMs from *Trpm2*$^{-/-}$ mice show a distinct phagosomal acidification defect. Phagosomal pH was determined by flow cytometry in BMDMs containing *SA*. (A) Histogram of flow cytometry measurements of *Trpm2*$^{+/+}$ BMDM containing *SA* conjugated to OG and TAMRA. pH-sensitive OG was excited at 488 nm and pH-insensitive TAMRA is excited at 561 nm under different pHs. The right shift of OG fluorescence is evident, but there is no change in TAMRA fluorescence, when pH changes from a lower (pH 4) to a higher (pH 7) value. (B) *In situ* calibration of pH with *SA* conjugate containing OG and TAMRA from measurements as described in A. Data are fitted to a Boltzmann equation. (C) Timecourse of phagosomal pH. In these experiments, *Trpm2*$^{+/+}$ and *Trpm2*$^{-/-}$ BMDMs are incubated with TAMRA and OG double-labeled *SA* as described in A for 10 min, and this is followed by flow cytometry measurements. Results are mean±s.e.m. (n=5). Phagosomal pH is determined based on the standard curve shown in B. *P<0.05 (t-test) as compared with BMDM. (D) NOX inhibition increased phagosomal pH. *Trpm2*$^{+/+}$ BMDMs treated with DPI showed an increased pH, similar to the pH observed in phagogomes of *Trpm2*$^{-/-}$ BMDMs treated with DPI (n=3). (E) Defective acidification impaired *PA* killing in BMDMs. BMDMs from *Trpm2*$^{+/+}$ and *Trpm2*$^{-/-}$ mice were pretreated with bafilomycin (0.1 µM) for 10 min before exposure to *PA* (MOI of 20) for 30 min and cultured for 120 min with the same concentration of bafilomycin at 37°C. Bars indicate mean±s.e.m. (n=3). *P<0.05 (t-test). (F,G) ADPR antagonism increases phagosomal pH and bacterial survival in *Trpm2*$^{+/+}$ BMDMs. BMDMs were pretreated with 8-Br-ADPR (10 µM) for 10 min at 37°C before exposure to *SA* conjugated to pH-sensitive OG and pH-insensitive TAMRA for pH measurements, or before they were exposed to *PA* for bacterial survival analysis. Bars indicate mean±s.e.m. (n=3, F; n=4, G). *n.s.*, not significant; *P<0.05 (t-test). (H) Model of oxidant-mediated TRPM2 activation regulating phagosomal acidification and bacterial killing. Upon bacterial challenge, NOX is activated and ROS are released. Oxidant stress results in increased formation of ADPR, which activates TRPM2. TRPM2 activations gates the flux of cations (Na^+ and Ca^{2+}) from phagosomes, which are regulated by cation concentrations (Lundqvist-Gustafsson et al., 2000) and phagosomal membrane potential (Steinberg et al., 2007b). Cation efflux (cation counter flux) and H^+ influx decreases phagosomal pH and thus favors bacterial killing.

(Knowles et al., 2011). The *Trpm2*$^{-/-}$ peritoneal macrophages, however, showed normal killing of *LM* (Knowles et al., 2011). In the present study, we clearly showed an essential role for TRPM2 localized in phagosomes for killing of both gram-positive bacteria *SA* and gram-negative bacteria *PA*. It appears from these disparate observations that the role of TRPM2 in mediating bacterial killing is complex. A possible explanation is that TRPM2-mediated bactericidal mechanisms vary depending on bacteria type, the state of activation of macrophages, the type of macrophages used for the study and the distinct functions of TRPM2 present in the plasmalemmal versus in the phagosome.

Our patch clamp results in isolated phagosomes showed the luminal orientation of the TRPM2 termini in phagosomes. That the N- and C-terminal regions of TRPM2 did not face the outer side of phagosomes suggests that phagosomal TRPM2 did not originate from the plasma membrane after phagocytosis. Phagosomal maturation requires spatial and temporal orchestration of proteins (for a review, see Levin et al., 2016). During the formation of phagosomes, proteins such as transferrin receptor are shuttled back to the plasma membrane whereas proteins such as the GTPase Rab5 are recruited into phagosomes (Levin et al., 2016). Other phagosomal proteins undergo retrograde traffic to the trans-Golgi network via tubulovesicular structures (Levin et al., 2016). The mechanism of TRPM2 positioning in phagosomes is not known. Our results on the timecourse of phagosome maturation showed that phagosomal TRPM2 activation and acidification occurred together, thus indicating that the recruitment of TRPM2 was directly coupled to phagosome maturation.

Journal of Cell Science (2017) 130, 735-744 doi:10.1242/jcs.196014

We also addressed the proximal basis of TRPM2 activation in phagosomes. Since TRPM2 is a redox-sensitive channel (Hara et al., 2002; Perraud et al., 2005), a possible mechanism of phagosomal TRPM2 activation may involve generation of oxidants and the subsequent production of ADPR (Hara et al., 2002; Knowles et al., 2013; Perraud et al., 2005; Syed Mortadza et al., 2015; Toth and Csanady, 2010; Wehage et al., 2002). We observed that the H_2O_2-activated current in *Trpm2*$^{+/+}$ BMDMs treated with an antagonistic analog of ADPR was reduced to the level seen in *Trpm2*$^{-/-}$ BMDMs, suggesting that H_2O_2 activated phagosomal TRPM2 through ADPR generation. The production of ADPR from mitochondria and nuclei (DNA) is considered to be primarily responsible for oxidative stress-induced TRPM2 activation (Hecquet and Malik, 2009). In phagosomes containing bacteria, DNA from nuclei may be the source for ROS-induced and NADase-mediated generation of ADPR (Bricker et al., 2002; Huang et al., 2009). Since NADase is ROS sensitive (Krapp et al., 1997; Ziegler et al., 1997), a tenable presumption is that H_2O_2 induces ADPR generation through activating NADase (Albeniz et al., 2004). This was confirmed by the observation that nicotinamide (an inhibitor of oxidant-sensitive NADase) (Alano et al., 2010) prevented H_2O_2-induced current, suggesting that ADPR generation in phagosomes involved the oxidant-sensitive transition of NAD into ADPR. Thus, our results support the model that ROS generation activated during phagocytosis mediated ADPR generation, and thereby signaled TRPM2 activation in phagosomes.

Phagosomes acquire an antimicrobial arsenal during the course of phagosomal maturation (Flannagan et al., 2009). This includes recruiting the vATPase that pumps H^+ into phagosomes, and assembly and activation of phagosomal membrane NADPH oxidases (NOXs) that produce ROS (Russell et al., 2009). In light of the role of ROS in bacteria killing (Pollock et al., 1995; Segal, 1996; Segal et al., 2000), the previous observation that the NOX-inhibiting function of TRPM2 promoted bacterial killing during phagocytosis at the plasma membrane (Di et al., 2011; Zhang et al., 2017) led us to consider the possibility that TRPM2 could also mediate bacterial killing through a phagosomal acidification mechanism. Phagosomal acidification in macrophages is essential for activation of lysosomal proteases, microbe killing and protein degradation (Aronson and De Duve, 1968; Coffey and De Duve, 1968; Pillay et al., 2002; Savina et al., 2006). The role of the ROS and NOX pathway in intra-phagosomal bacterial killing has been proposed in part based on findings in chronic granulomatous disease (CGD) (Pollock et al., 1995; Segal, 1996; Segal et al., 2000). CDG is characterized by severe, protracted and fatal infection resulting from the failure of the NOX system to produce superoxide (O_2^-) and other ROS in neutrophils (Pollock et al., 1995; Segal, 1996; Segal et al., 2000); however, it was later discovered that defective bacterial killing in CGD neutrophils was secondary to dysregulated phagosomal acidification mechanism (Dri et al., 2002; Geiszt et al., 2001; Henriet et al., 2013; Segal et al., 1981; Thrasher and Segal, 2011). We previously showed that TRPM2 inhibited NOX-mediated ROS generation, specifically that there was overproduction of ROS in *Trpm2*$^{-/-}$ macrophages infected with *E. coli* (Di et al., 2011). In the present study, however, DPI treatment of *Trpm2*$^{-/-}$ mBMDMs failed to alter significantly phagosomal pH, indicating that the increased pH seen in *Trpm2*$^{-/-}$ mBMDMs was caused by TRPM2 deletion rather than increased ROS production secondary to TRPM2 deletion (Di et al., 2011). Thus, the dysregulated phagosomal pH in *Trpm2*$^{-/-}$ BMDMs, as opposed to the overproduction of ROS, was essential for the phagosomal killing of bacteria as was shown to be the case for CDG neutrophils (Dri et al., 2002; Geiszt et al., 2001; Henriet et al., 2013; Segal et al., 1981; Thrasher and Segal, 2011).

In summary, we demonstrated that TRPM2 localized in phagosomes is required for mediating bacterial killing through facilitating acidification of phagosomes in macrophages. This finding suggests that strategies aimed at activating TRPM2-mediated cation efflux, such as through ADPR generation, might enhance acidification and thereby the bactericidal function of macrophage.

MATERIALS AND METHODS

Mice

Age (4–6 weeks)- and sex (both male and female)-matched mice were used in these studies. TRPM2-knockout (*Trpm2*$^{-/-}$) mice used in these studies were generously provided by Dr. Yasuo Mori (Department of Technology and Ecology, Kyoto University, Japan; Yamamoto et al., 2008); these mice were generated by deleting exons corresponding to transmembrane (TM) spans 5 and 6, including the pore loop. C57BL6 mice were obtained from Charles River Laboratory. All mice were housed in the University of Illinois Animal Care Facility in accordance with institutional and NIH guidelines. All experiments were approved by the University of Illinois Animal Resources Center.

Cell culture and reagents

Mouse bone marrow-derived macrophages (mBMDMs) were induced and cultured as described previously (Zhang et al., 2008). *Pseudomonas aeruginosa* (*PA*) strain 103, was a gift from Dr Yuru Liu (University of Illinois, Chicago, IL) and *Staphylococcus aureus* strain USA 300 (*SA*) was a gift from Dr Nancy Freitag (University of Illinois, Chicago, IL). Bacteria were suspended in medium containing 20% glycerol, and frozen in aliquots at −70°C. Before each experiment, an aliquot was thawed and cultured in Luria-Bertani (LB) broth at 37°C with continuous shaking, and the exact number of bacteria was determined by plating serial dilutions onto LB agar plates for overnight culture. The original culture was kept at 4°C and was used for infection once the concentration of live bacteria was determined overnight (~12 h). Unlabeled *SA* (Wood strain without protein A) bio-particles (*SA*, S-2859), Oregon Green 488 carboxylic acid succinimidyl ester (OG, O6149), 6-carboxy-tetramethyl-rhodamine (TAMRA, C6122), Fluo3-AM (F-14218), Fluo-3 pentapotassium salt (F3715) and pHrodo (A10010) were purchased from Life Technologies (NY). Rabbit anti-human TRPM2 antibody (ab11168) was purchased from Abcam (MA, USA) and used at 1:100. 8-Br-ADPR (B 051-05) was purchased from Biolog/Axxora, LLC (Enzo Life Sciences, Inc.). Bafilomycin (B1793), latex beads (3.0 µm, LB30), Nicotinamide (N3376) and other chemicals were purchased from Sigma (MO).

Human cell experiments

Use of human subjects for broncho-alveolar lavage was approved by the Institutional Review Board of University of Illinois Chicago Hospitals (Chicago, IL). Informed consent was obtained for all tissue donors and all clinical investigation have been conducted according to the principles expressed in the Declaration of Helsinki.

Polymicrobial sepsis model and survival

Mouse polymicrobial sepsis was induced by cecal ligation puncture (CLP) as described previously (Cuenca et al., 2010) using a 16-gauge needle. For survival studies, mice were monitored twice daily for 6 days.

Lung infection model, survival in mice, and lung bactericidal activity

Lung infection with *PA* was induced by intra-tracheal administration of *PA* (10^5 in 30 µl). For survival studies, mice were monitored twice daily for 6 days after *PA* administration. Bactericidal activity in lungs was assessed as described previously (Sadikot et al., 2006). Mice were killed and lungs were removed 48 h after *PA* administration. The lung was removed aseptically and placed in 1 ml of sterile HBSS. Lungs were homogenized in a tissue

homogenizer in a vented hood under sterile conditions. Serial dilutions of the homogenates were made and 10 µl of each dilution were plated in agar plates. Plates were incubated for 18 h at 37°C, and the number of *PA* colonies was counted.

Bactericidal activity assay

Bactericidal activity of macrophage was analyzed by performing a colony-forming unit (CFU) assay as described previously (Hamrick et al., 2000). *Pseudomonas aeruginosa* strain 103 (*PA*) and *Staphylococcus aureus* strain USA 300 (*SA*) were grown in tryptic soy broth for 14 h at 37°C, and bacteria concentrations were determined by serial dilutions and counting CFUs. In each sample, 2×10^5 macrophages on culture dishes were infected with bacteria at a multiplicity of infection (MOI) of 20 for *PA* or an MOI of 10 for *SA* for 30 min at 37°C. Cells were gently scraped off the bottom of the culture dish into the medium and centrifuged at 500 ***g*** for 10 min at 4°C. Then, supernatant was aspirated and pellets were re-suspended in DMEM with 10% fetal bovine serum (FBS). Non-internalized bacteria were killed by adding 100 µg/ml gentamicin to the medium and incubating for 1 h at 37°C. It was tested that a 1 h pulse with gentamicin is sufficient to kill these bacteria. Samples were centrifuged (500 ***g*** for 10 min), and the pellets re-suspended in medium with 10 µg/ml gentamicin. Macrophage bactericidal activity was monitored at 37°C over several time points (0, 2 or 3 h). At each time point, cells were centrifuged at 500 ***g*** for 5 min and the cell pellet was re-suspended in 1% Triton X-100 in PBS. Cells were lysed for 2 min at room temperature (RT) and 50, 100 and 500 µl aliquots of lysate were spread onto agar plates. Surviving bacteria were grown for 16 h and the number of colony-forming units was tabulated.

TRPM2 immunostaining of macrophages loaded with beads

Bone marrow-derived macrophage (BMDMs) from both *Trpm2*$^{-/-}$ and *Trpm2*$^{+/+}$ mice plated on 25 mm coverslips were treated with 3 µm latex beads at 37°C for 30 min. Phagocytosis was stopped by transferring coverslips to ice-cold PBS, and washing five times with PBS to remove any remaining external beads, and fixed for 20 min in 3% paraformaldehyde in HBBS. Macrophages were stained with anti-TRPM2 antibody for 1 h and localization of TRPM2 and phagocytosed beads were imaged with a Zeiss LSM 710 confocal microscope using 488 and 561 nm lasers and a 63× objective lens (NA 1.3). Images were acquired with LCS software and images were processed with Fiji software.

Phagosome current recording

Whole phagosomal current was measured as described previously (Samie et al., 2013). Red blood cells (RBCs) opsonized with IgG were incubated with BMDMs at 37°C and 5% CO_2 for 10 min to lead to the formation of phagosomes. To release phagosomes from cells, a patch pipette was used to open the cell by slicing the cell membrane. Currents from the isolated phagosome were elicited using a series of test pulses ranging from −110 to +110 mV (test pulses were 200 ms in duration and delivered at 2 s intervals). The holding potential was 0 mV. The pipette solution contained (in mM): 135 $CsSO_3CH_3$, 8 NaCl, 2 $MgCl_2$, 0.5 $CaCl_2$, 1 EGTA and 10 HEPES pH 7.4. ADPR (200 µM) or H_2O_2 (100 µM) was included in the pipette solution to induce TRPM2 current. The bath solution contained (in mM): 145 NaCl, 2 $CaCl_2$, 1 MgC_2 and 10 HEPES pH 7.4. Phagosomal current was analyzed using IGOR software (WaveMetrics, Lake Oswego, OR).

Determination of phagosomal acidification

Acidification of phagosomes containing *SA* was measured as described previously (Sokolovska et al., 2012). *SA* was labeled with both OG and TAMRA as above. Macrophages were cultured on a 96-well plate (Nunclon Delta surface, Thermo Scientific) at a concentration of 5×10^5 cells/well, and were incubated with labeled *SA* particles at a MOI of 5 for 10 min at 37°C for flow cytometry analysis. The ratio of the mean fluorescence from OG over mean fluorescence of TAMRA was determined by flow cytometry (LSR Fortessa, BD, NJ) with a 488 nm and a 561 nm laser. The intra-phagosome pH values were interpolated on a standard curve for *SA* fluorescence versus pH determined *in vitro* using a series of buffers as above. For phagosomal pH calibration, phagosomal pH was equalized by incubating cells for 15–20 min at 37°C in calibration buffer (120 mM KCl, 20 mM NaCl, 1 mM $CaCl_2$, 1 mM $MgCl_2$, 10 mM HEPES with the pH adjusted from 4 to 8) containing the ionophores carbonyl cyanide m-chlorophenylhydrazone (CCCP, 10 µM), nigericin (10 µM) and the H^+ vATPase pump inhibitor bafilomycin (0.1 µM). Changes in pH were measured by assessing the intensity ratio of OG to TAMRA in each phagosome. OG:TAMRA ratios were plotted against pH values and curves were fitted with the sigmoidal Boltzman equation. In each independent experiment, results from three samples (each containing about 5×10^5 cells) of the same group were averaged, and averaged results from six independent experiments (n=6) were presented.

Simultaneous recording of phagosomal TRPM2 activation and acidification during phagosome maturation

Cellular and intra-phagosomal Ca^{2+} was monitored with fluo3 as the Ca^{2+} indicator (Minta et al., 1989), and phagosomal acidification was monitored by using the pH-sensitive fluorescent dye pHrodo conjugated to *SA*. BMDMs from both *Trpm2*$^{+/+}$ and *Trpm2*$^{-/-}$ were first loaded with 5 µM fluo3-AM (membrane permeant) for 30 min at 37°C and cells were then infected with *SA* conjugated to the pH-sensitive fluorescent dye pHrodo (Han and Burgess, 2010) with a MOI of 10. The pHrodo dye has the property that its fluorescence increases as pH decreases from neutral to acidic (Inc., 2014); however, importantly it does not fluorescence outside the cell (Miksa et al., 2009) and therefore is useful in identifying particles internalized in phagosomes. Dye emission was determined with a Zeiss LSM 710 confocal microscope by using a 488 nm and a 561 nm laser, a 63× objective lens (NA 1.3) and an emission bandwidth of 500–535 nm and 600–680 mm. Images were collected every 10 s with LCS software and were processed and analyzed with Fiji software.

Data analysis and statistics

Images were analyzed using Fiji software (NIH). Summary data are expressed as mean±s.e.m. with the number of experiments listed in parentheses or indicated in the text. Significance between groups was determined using the Student's *t*-test (two-tailed) and asterisks indicate values as shown.

Acknowledgements

We thank Dr Sergio Grinstein of Hospital for Sick Children and Nic Demaraux of University of Geneva for insights into the work and Dr Balaji Ganesh (University of Illinois at Chicago) for flow cytometry experiment design and data analysis.

Competing interests

The authors declare no competing or financial interests.

Author contributions

A.D. and A.B.M. designed the study; A.D., T.Y., H.G. and X.G. performed experiments and data analysis; A.D. and A.B.M. wrote the paper with input from the other authors.

Funding

This work was supported by the National Institutes of Health (P01HL77806). T.K. was supported by Saiseikai Otaru Hospital, Japan. Deposited in PMC for release after 12 months.

Supplementary information

Supplementary information available online at
http://jcs.biologists.org/lookup/doi/10.1242/jcs.196014.supplemental

References

Alano, C. C., Garnier, P., Ying, W., Higashi, Y., Kauppinen, T. M. and Swanson, R. A. (2010). NAD+ depletion is necessary and sufficient for poly (ADP-ribose) polymerase-1-mediated neuronal death. *J. Neurosci.* **30**, 2967-2978.

Albeniz, I., Demir, O., Nurten, R. and Bermek, E. (2004). NAD glycohydrolase activities and ADP-ribose uptake in erythrocytes from normal subjects and cancer patients. *Biosci. Rep.* **24**, 41-53.

Aronson, N. N., Jr and De Duve, C. (1968). Digestive activity of lysosomes. II. The digestion of macromolecular carbohydrates by extracts of rat liver lysosomes. *J. Biol. Chem.* **243**, 4564-4573.

Bricker, A. L., Cywes, C., Ashbaugh, C. D. and Wessels, M. R. (2002). NAD +-glycohydrolase acts as an intracellular toxin to enhance the extracellular survival of group A streptococci. *Mol. Microbiol.* **44**, 257-269.

Coffey, J. W. and De Duve, C. (1968). Digestive activity of lysosomes. I. The digestion of proteins by extracts of rat liver lysosomes. *J. Biol. Chem.* **243**, 3255-3263.
Cross, A. R. and Jones, O. T. (1986). The effect of the inhibitor diphenylene iodonium on the superoxide-generating system of neutrophils. Specific labelling of a component polypeptide of the oxidase. *Biochem. J.* **237**, 111-116.
Cuenca, A. G., Delano, M. J., Kelly-Scumpia, K. M., Moldawer, L. L., Efron, P. A. (2010). Cecal ligation and puncture. *Curr. Protoc. Immunol.* Chapter 19, Unit 19 13.
Di, A., Gao, X.-P., Qian, F., Kawamura, T., Han, J., Hecquet, C., Ye, R. D., Vogel, S. M. and Malik, A. B. (2011). The redox-sensitive cation channel TRPM2 modulates phagocyte ROS production and inflammation. *Nat. Immunol.* **13**, 29-34.
Dri, P., Presani, G., Perticarari, S., Albèri, L., Prodan, M. and Decleva, E. (2002). Measurement of phagosomal pH of normal and CGD-like human neutrophils by dual fluorescence flow cytometry. *Cytometry* **48**, 159-166.
Flannagan, R. S., Cosio, G. and Grinstein, S. (2009). Antimicrobial mechanisms of phagocytes and bacterial evasion strategies. *Nat. Rev. Microbiol.* **7**, 355-366.
Fonfria, E., Marshall, I. C., Benham, C. D., Boyfield, I., Brown, J. D., Hill, K., Hughes, J. P., Skaper, S. D. and McNulty, S. (2004). TRPM2 channel opening in response to oxidative stress is dependent on activation of poly(ADP-ribose) polymerase. *Br. J. Pharmacol.* **143**, 186-192.
Geiszt, M., Kapus, A. and Ligeti, E. (2001). Chronic granulomatous disease: more than the lack of superoxide? *J. Leukoc. Biol.* **69**, 191-196.
Hamrick, T. S., Havell, E. A., Horton, J. R. and Orndorff, P. E. (2000). Host and bacterial factors involved in the innate ability of mouse macrophages to eliminate internalized unopsonized Escherichia coli. *Infect. Immun.* **68**, 125-132.
Han, J. and Burgess, K. (2010). Fluorescent indicators for intracellular pH. *Chem. Rev.* **110**, 2709-2728.
Hara, Y., Wakamori, M., Ishii, M., Maeno, E., Nishida, M., Yoshida, T., Yamada, H., Shimizu, S., Mori, E., Kudoh, J. et al. (2002). LTRPC2 Ca2+-permeable channel activated by changes in redox status confers susceptibility to cell death. *Mol. Cell* **9**, 163-173.
Hara-Chikuma, M., Yang, B., Sonawane, N. D., Sasaki, S., Uchida, S. and Verkman, A. S. (2005). ClC-3 chloride channels facilitate endosomal acidification and chloride accumulation. *J. Biol. Chem.* **280**, 1241-1247.
Hecquet, C. M. and Malik, A. B. (2009). Role of H(2)O(2)-activated TRPM2 calcium channel in oxidant-induced endothelial injury. *Thromb. Haemost.* **101**, 619-625.
Henriet, S. S., Jans, J., Simonetti, E., Kwon-Chung, K. J., Rijs, A. J. M. M., Hermans, P. W. M., Holland, S. M., de Jonge, M. I. and Warris, A. (2013). Chloroquine modulates the fungal immune response in phagocytic cells from patients with chronic granulomatous disease. *J. Infect. Dis.* **207**, 1932-1939.
Huang, N., De Ingeniis, J., Galeazzi, L., Mancini, C., Korostelev, Y. D., Rakhmaninova, A. B., Gelfand, M. S., Rodionov, D. A., Raffaelli, N. and Zhang, H. (2009). Structure and function of an ADP-ribose-dependent transcriptional regulator of NAD metabolism. *Structure* **17**, 939-951.
Kinchen, J. M. and Ravichandran, K. S. (2008). Phagosome maturation: going through the acid test. *Nat. Rev. Mol. Cell Biol.* **9**, 781-795.
Knowles, H., Heizer, J. W., Li, Y., Chapman, K., Ogden, C. A., Andreasen, K., Shapland, E., Kucera, G., Mogan, J., Humann, J. et al. (2011). Transient receptor potential melastatin 2 (TRPM2) ion channel is required for innate immunity against Listeria monocytogenes. *Proc. Natl. Acad. Sci. USA* **108**, 11578-11583.
Knowles, H., Li, Y. and Perraud, A.-L. (2013). The TRPM2 ion channel, an oxidative stress and metabolic sensor regulating innate immunity and inflammation. *Immunol. Res.* **55**, 241-248.
Krapp, A. R., Tognetti, V. B., Carrillo, N. and Acevedo, A. (1997). The role of ferredoxin-NADP+ reductase in the concerted cell defense against oxidative damage – studies using Escherichia coli mutants and cloned plant genes. *Eur. J. Biochem.* **249**, 556-563.
Levin, R., Grinstein, S. and Canton, J. (2016). The life cycle of phagosomes: formation, maturation, and resolution. *Immunol. Rev.* **273**, 156-179.
Lukacs, G. L., Rotstein, O. D. and Grinstein, S. (1990). Phagosomal acidification is mediated by a vacuolar-type H(+)-ATPase in murine macrophages. *J. Biol. Chem.* **265**, 21099-21107.
Lundqvist-Gustafsson, H., Gustafsson, M. and Dahlgren, C. (2000). Dynamic ca (2+)changes in neutrophil phagosomes A source for intracellular ca(2+)during phagolysosome formation? *Cell Calcium* **27**, 353-362.
Meikle, P. J., Brooks, D. A., Ravenscroft, E. M., Yan, M., Williams, R. E., Jaunzems, A. E., Chataway, T. K., Karageorgos, L. E., Davey, R. C., Boulter, C. D. et al. (1997). Diagnosis of lysosomal storage disorders: evaluation of lysosome-associated membrane protein LAMP-1 as a diagnostic marker. *Clin. Chem.* **43**, 1325-1335.
Miksa, M., Komura, H., Wu, R., Shah, K. G. and Wang, P. (2009). A novel method to determine the engulfment of apoptotic cells by macrophages using pHrodo succinimidyl ester. *J. Immunol. Methods* **342**, 71-77.
Minta, A., Kao, J. P. and Tsien, R. Y. (1989). Fluorescent indicators for cytosolic calcium based on rhodamine and fluorescein chromophores. *J. Biol. Chem.* **264**, 8171-8178.
Partida-Sanchez, S., Gasser, A., Fliegert, R., Siebrands, C. C., Dammermann, W., Shi, G., Mousseau, B. J., Sumoza-Toledo, A., Bhagat, H., Walseth, T. F. et al. (2007). Chemotaxis of mouse bone marrow neutrophils and dendritic cells is controlled by adp-ribose, the major product generated by the CD38 enzyme reaction. *J. Immunol.* **179**, 7827-7839.
Perraud, A. L., Fleig, A., Dunn, C. A., Bagley, L. A., Launay, P., Schmitz, C., Stokes, A. J., Zhu, Q., Bessman, M. J., Penner, R. et al. (2001). ADP-ribose gating of the calcium-permeable LTRPC2 channel revealed by Nudix motif homology. *Nature* **411**, 595-599.
Perraud, A. L., Takanishi, C. L., Shen, B., Kang, S., Smith, M. K., Schmitz, C., Knowles, H. M., Ferraris, D., Li, W., Zhang, J. et al. (2005). Accumulation of free ADP-ribose from mitochondria mediates oxidative stress-induced gating of TRPM2 cation channels. *J. Biol. Chem.* **280**, 6138-6148.
Pillay, C. S., Elliott, E. and Dennison, C. (2002). Endolysosomal proteolysis and its regulation. *Biochem. J.* **363**, 417-429.
Pollock, J. D., Williams, D. A., Gifford, M. A., Li, L. L., Du, X., Fisherman, J., Orkin, S. H., Doerschuk, C. M. and Dinauer, M. C. (1995). Mouse model of X-linked chronic granulomatous disease, an inherited defect in phagocyte superoxide production. *Nat. Genet.* **9**, 202-209.
Qian, X., Numata, T., Zhang, K., Li, C., Hou, J., Mori, Y. and Fang, X. (2014). Transient receptor potential melastatin 2 protects mice against polymicrobial sepsis by enhancing bacterial clearance. *Anesthesiology* **121**, 336-351.
Russell, D. G., Vanderven, B. C., Glennie, S., Mwandumba, H. and Heyderman, R. S. (2009). The macrophage marches on its phagosome: dynamic assays of phagosome function. *Nat. Rev. Immunol.* **9**, 594-600.
Sadikot, R. T., Blackwell, T. S., Christman, J. W. and Prince, A. S. (2005). Pathogen-host interactions in Pseudomonas aeruginosa pneumonia. *Am. J. Respir. Crit. Care. Med.* **171**, 1209-1223.
Sadikot, R. T., Zeng, H., Joo, M., Everhart, M. B., Sherrill, T. P., Li, B., Cheng, D. S., Yull, F. E., Christman, J. W. and Blackwell, T. S. (2006). Targeted immunomodulation of the NF-kappaB pathway in airway epithelium impacts host defense against Pseudomonas aeruginosa. *J. Immunol.* **176**, 4923-4930.
Samie, M., Wang, X., Zhang, X., Goschka, A., Li, X., Cheng, X., Gregg, E., Azar, M., Zhuo, Y., Garrity, A. G. et al. (2013). A TRP channel in the lysosome regulates large particle phagocytosis via focal exocytosis. *Dev. Cell* **26**, 511-524.
Savina, A., Jancic, C., Hugues, S., Guermonprez, P., Vargas, P., Moura, I. C., Lennon-Dumenil, A. M., Seabra, M. C., Raposo, G. and Amigorena, S. (2006). NOX2 controls phagosomal pH to regulate antigen processing during crosspresentation by dendritic cells. *Cell* **126**, 205-218.
Segal, A. W. (1996). The NADPH oxidase and chronic granulomatous disease. *Mol. Med. Today* **2**, 129-135.
Segal, A. W., Geisow, M., Garcia, R., Harper, A. and Miller, R. (1981). The respiratory burst of phagocytic cells is associated with a rise in vacuolar pH. *Nature* **290**, 406-409.
Segal, B. H., Leto, T. L., Gallin, J. I., Malech, H. L. and Holland, S. M. (2000). Genetic, biochemical, and clinical features of chronic granulomatous disease. *Medicine* **79**, 170-200.
Sokolovska, A., Becker, C. E. and Stuart, L. M. (2012). Measurement of phagocytosis, phagosome acidification, and intracellular killing of Staphylococcus aureus. *Curr. Protoc. Immunol.* Chapter 14, Unit14 30.
Steinberg, B. E., Huynh, K. K. and Grinstein, S. (2007a). Phagosomal acidification: measurement, manipulation and functional consequences. *Biochem. Soc. Trans.* **35**, 1083-1087.
Steinberg, B. E., Touret, N., Vargas-Caballero, M. and Grinstein, S. (2007b). In situ measurement of the electrical potential across the phagosomal membrane using FRET and its contribution to the proton-motive force. *Proc. Natl. Acad. Sci. USA* **104**, 9523-9528.
Steinberg, B. E., Huynh, K. K., Brodovitch, A., Jabs, S., Stauber, T., Jentsch, T. J. and Grinstein, S. (2010). A cation counterflux supports lysosomal acidification. *J. Cell Biol.* **189**, 1171-1186.
Syed Mortadza, S. A., Wang, L., Li, D. and Jiang, L. H. (2015). TRPM2 channel-mediated ROS-sensitive Ca(2+) signaling mechanisms in immune cells. *Front. Immunol.* **6**, 407.
Thrasher, A. J. and Segal, A. W. (2011). A phagocyte dilemma. *Nat. Immunol.* **12**, 201-202.
Toth, B. and Csanady, L. (2010). Identification of direct and indirect effectors of the transient receptor potential melastatin 2 (TRPM2) cation channel. *J. Biol. Chem.* **285**, 30091-30102.
Vieira, O. V., Botelho, R. J. and Grinstein, S. (2002). Phagosome maturation: aging gracefully. *Biochem. J.* **366**, 689-704.
Wehage, E., Eisfeld, J., Heiner, I., Jüngling, E., Zitt, C. and Luckhoff, A. (2002). Activation of the cation channel long transient receptor potential channel 2 (LTRPC2) by hydrogen peroxide. A splice variant reveals a mode of activation independent of ADP-ribose. *J. Biol. Chem.* **277**, 23150-23156.
Yamamoto, S., Shimizu, S., Kiyonaka, S., Takahashi, N., Wajima, T., Hara, Y., Negoro, T., Hiroi, T., Kiuchi, Y., Okada, T. et al. (2008). TRPM2-mediated Ca2+influx induces chemokine production in monocytes that aggravates inflammatory neutrophil infiltration. *Nat. Med.* **14**, 738-747.

Zhang, X., Goncalves, R. and Mosser, D. M. (2008). The isolation and characterization of murine macrophages. *Curr. Protoc. Immunol.* Chapter 14, Unit 14 11.

Zhang, Z., Cui, P., Zhang, K., Chen, Q. and Fang, X. (2017). Transient receptor potential melastatin 2 regulates phagosome maturation and is required for bacterial clearance in Escherichia coli sepsis. *Anesthesiology*. 126, 128-139.

Ziegler, M., Jorcke, D. and Schweiger, M. (1997). Identification of bovine liver mitochondrial NAD+ glycohydrolase as ADP-ribosyl cyclase. *Biochem. J.* **326**, 401-405.